On the formation of lines in quantum phase space

OPEN ACCESS
IOP Publishing
Journal of Physics A: Mathematical and Theoretical
J. Phys. A: Math. Theor. **56** (2023) 015306 (16pp)
https://doi.org/10.1088/1751-8121/acaa98

On the formation of lines in quantum phase space

Ole Steuernagel[1,2,*], **Popo Yang**[2] and **Ray-Kuang Lee**[2,3,4,5]

[1] Department of Physics, Astronomy and Mathematics, University of Hertfordshire, Hatfield AL10 9AB, United Kingdom
[2] Institute of Photonics Technologies, National Tsing Hua University, Hsinchu 30013, Taiwan
[3] Department of Physics, National Tsing Hua University, Hsinchu 30013, Taiwan
[4] Physics Division, National Center for Theoretical Sciences, Taipei 10617, Taiwan
[5] Center for Quantum Technology, Hsinchu 30013, Taiwan

E-mail: Ole.Steuernagel@gmail.com

Received 26 August 2022; revised 11 November 2022
Accepted for publication 12 December 2022
Published 24 January 2023

Abstract

We theoretically study the formation of lines in phase space using Wigner's distribution W. In trapped quantum systems such lines form generically, crisscrossing phase space and they can have astonishing extent, reaching across the entire state. In classical systems this does not happen. We show that the formation of such straight line patterns is due to the formation of 'randomized comb-states'. We establish their stability to perturbations, and that they are tied to coherences in configuration space. We additionally identify generic higher-order 'eye' patterns in phase space which occur less often since they arise from more specific symmetric comb-states; we show that the perturbation of eye patterns through their randomization tends to deform them into lines. Lines in phase space should give rise to large probability peaks in measurements.

Keywords: quantum phase space, Wigner distribution, nonlinear Schrödinger equation, lines in phase space

(Some figures may appear in colour only in the online journal)

* Author to whom any correspondence should be addressed.

1. Introduction

Quantum waves frequently form long lines in phase space. This has not been reported before [1–6], and is astonishing when viewed from the perspective of classical phase space densities.

To study phase space behaviour we map the quantum waves ψ onto their associated Wigner distribution, W [7]. While time evolves, W forms lines and does so repeatedly. The lines crisscross W, often in such a way that they reach across the entire distribution. This trend, to form lines in phase space, is enhanced by attractive and suppressed by repulsive nonlinear interactions of ψ.

We note that such straight lines should create significant peaks detectable in (rotated quadrature) measurements, as used in quantum [8] or atom optical [9] experiments measuring projections of W.

Formally, we study one-dimensional single-particle quantum waves $\psi(x,t)$, in position x and time t, whose evolution obeys linear or nonlinear Schrödinger equations (NLSEs) [10] of the form

$$i\frac{\partial\psi}{\partial t} = -\frac{1}{2}\frac{\partial^2\psi}{\partial x^2} + V(x)\psi - \gamma(t)|\psi|^\epsilon\psi\ . \tag{1}$$

We always assume either the conservative potential $V(x)$ to be trapping, or the nonlinear (energy conserving) interactions to be self-attracting ($\gamma > 0$).

Such attractive nonlinear interactions describe multi-particle or field phenomena which can lead to the formation, stabilization and interaction of pulses in plasmas [11], nonlinear optics [12] or dilute ultracold clouds of atoms, and the generation of rogue waves [13], tidal bores, dam break scenarios [14] and many other nonlinear wave phenomena [15]. For order $\epsilon = 2$ [16], equation (1) is also known as the Gross–Pitaevskii equation.

Few analytical solutions for NLSEs (1) are known and generally little is established about the generic behaviour of solutions for arbitrary initial states and in the presence of external potentials. We numerically investigate their phase space behaviour, showing that they often form straight lines crisscrossing phase space and also 'eye' patterns for a large variety of different scenarios, different initial states, different confining potentials and different classes of NLSEs of varying order $\epsilon + 1$ and strength γ of their nonlinearity.

In this work, after we remind ourselves of the behaviour of classical systems, in the next paragraph, we introduce Wigner's distribution in section 2, then we will concentrate on the dynamics of the linear Schrödinger equation of quantum mechanics for a trapped system in section 3. In section 4, we show that the formation of (positive) straight lines in phase space is due to the formation of randomized comb-states, whereas eye patterns are due to more symmetrical comb-states with locally concave or convex arrangements of the weights of their peaks. Finally, we consider nonlinear systems without trapping potential in section 5.1 followed by nonlinear systems with trapping potential in section 5.2.

1.1. Classical systems:

Spread-out states subjected to conservative Hamiltonian time evolution in classical phase space, typically, form delicate folded patterns on ever smaller scales as the Hamiltonian flow stretches and folds their (initially concentrated, but non-singular) distributions. Similar whorl patterns can also form in the quantum case [1], at least temporarily, but they are limited by a minimum scale first identified by Zurek [4, 17].

Lines in classical phase space can arise for free particles with distributions initially spatially concentrated as their nonzero momentum spread over time induces an unlimited affine shear in phase space [9]. Systems *isomorphic* to free particles, namely, when $V(x)$ forms linear ramps or harmonic traps induce purely classical transport [18, 19]. This can result in displacements, rotations and shearing but does not at all change W's interference patterns in phase space [18, 19]. Being in this sense trivial we will not discuss such cases any further.

For systems confined by a non-harmonic trapping potential, lines do not form in classical phase space unless one starts out with special initial states (back-propagated line states). Such lines then form once but not again.

In the quantum case we find the dynamics creates lines in many different scenarios, in view of the classical behaviours this is puzzling and demands an explanation. We will show that these lines in phase space are created by the coherences of randomized comb-states. More symmetrical comb-states can create ringed 'eye' patterns, upon perturbation such eye patterns morph into lines.

2. Wigner's distribution

Here, we do not assume periodic boundary conditions thus avoiding quantization of momentum into discrete momentum modes [22, 23].

To study phase space behaviour for equation (1) we determine ψ's Wigner distribution W [24] associated with pure states $\psi(x,t)$ [25], namely

$$W(x,p,t) = \frac{1}{\pi}\int_{-\infty}^{\infty} \mathrm{d}y\, \psi(x+y,t)\psi^*(x-y,t)\mathrm{e}^{-2ipy}. \tag{2}$$

W is a function of x, t and momentum p and known to fully represent all information contained in ψ. By construction W is nonlocal (through y) and normalized: $\int \mathrm{d}p \int \mathrm{d}x\, W(x,p,t) = 1$. Unlike ψ, W is always real-valued but features negative regions [7] and is thus considered a distribution featuring 'quasi-probabilities' [26].

Here, we consider 1D problems and always assume wave functions to be normalized $\int |\psi(x,t)|^2 \mathrm{d}x = 1$.

The projections of W yield the densities in position $P(x,t) = |\psi(x,t)|^2 = \int \mathrm{d}p\, W(x,p,t)$ and in momentum $\tilde{P}(p,t) = |\tilde{\psi}(p,t)|^2 = \int \mathrm{d}x\, W(x,p,t)$, respectively. Thus, long straight lines, reaching across entire distributions, can only form when they have *positive* values.

3. Trapped linear systems

We find that trapped systems sooner or later form lines in phase space. When we choose a spatially concentrated initial state, the (anharmonic) potential $V(x)$ disperses the state over its energy corridor in phase space (the black background lines in figures 1 and 2 depict energy contours). This process has to happen first until finally the state is sufficiently dispersed to self-interfere as irregular standing waves, i.e. form random comb-states, see (b)–(d) and, to a lesser extent, (B)–(D) in figure 1.

These random comb-states are responsible for the formation of lines in phase space, see section 4.

Simple enough trapped systems can show state revivals after a 'recurrence' or 'revival' time T_r (at $t = T_\mathrm{r}$ the evolved state is identical to the initial state [27] or very similar to it [17, 20, 21]). For such, not too highly excited linear systems T_r can be so short that we can study it numerically. At suitable fractions of T_r, namely, at times of 'fractional revivals' of the initial

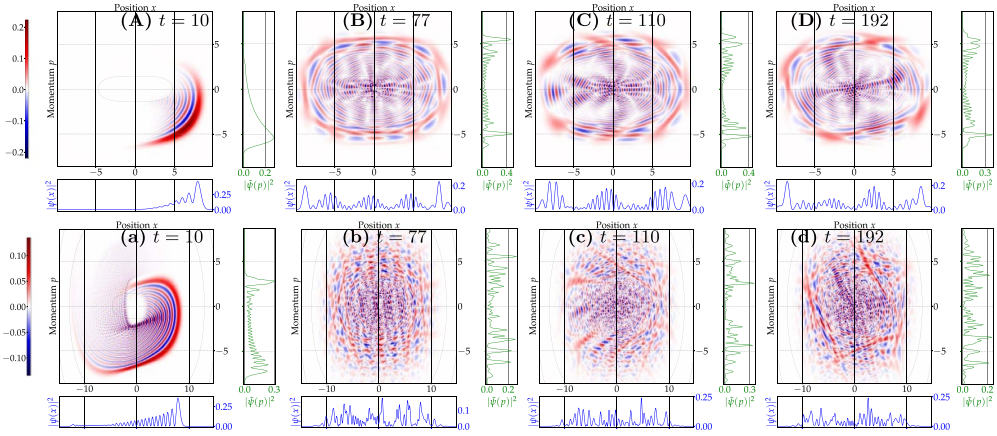

Figure 1. The Wigner distribution evolved in a linear system with potential $V(x) = x^4/500$, has a recurrence time [20, 21] $T_\mathrm{r} \approx 750$ at which the evolved state roughly reforms [17]. For the top row, (A)–(D), the initial state $\psi_0 = (2/\pi)^{1/4}\exp[-(x-9)^2]$ is used; for the bottom row, (a)–(d), the initial state is more squeezed in p: $\psi_0 = (2/9\pi)^{1/4}\exp[-(x-9)^2/9]$. For short times (A) and (a) the state forms a fringed crescent. At greater times the distribution covers its energy corridor in phase space and around $t = 77$, (B) and (b), straight lines first appear. Such straight lines tend to have larger extent in cases where the state covers a larger area in phase space, (c) versus (C). At time $t = 192 \approx T_\mathrm{r}/4$, (D) and (d), fractional revivals of the initial state with approximately fourfold symmetry form [17, 20, 21].

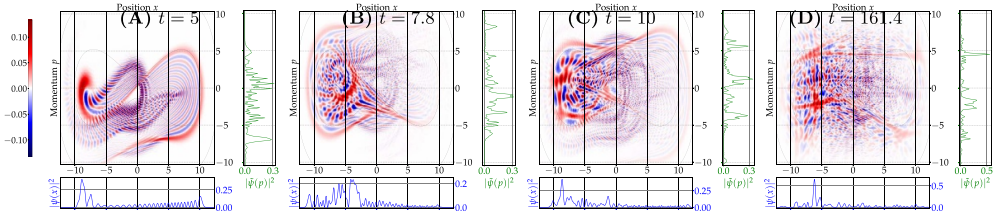

Figure 2. Wigner distributions evolved in double well potential $V(x) = x^4/200 - x^2/2$. The initial state $\psi_0 = (2/5\pi)^{1/4}\exp[-(x+9.9)^2/5]$ has an energy that partly exceeds the central barrier as can be seen clearly at short times (A). Subsequently, lines form quite soon (B) and keep reappearing (C)-(D).

state [17, 20, 21, 27], we witness pronounced formation of lines in phase space, for an example see figures 1(D) and (d).

4. Comb-states have to be random to form lines in phase space

The formation of (positive) straight lines in phase space is due to the formation of randomized comb-states. If the comb-states are too symmetrical, they form higher order concentric ring or 'eye' patterns, instead of lines. These eye patterns are most pronounced for comb-states with locally concave or convex arrangements of the weights of their peaks. We now give numerical and semi-analytical evidence to support these claims.

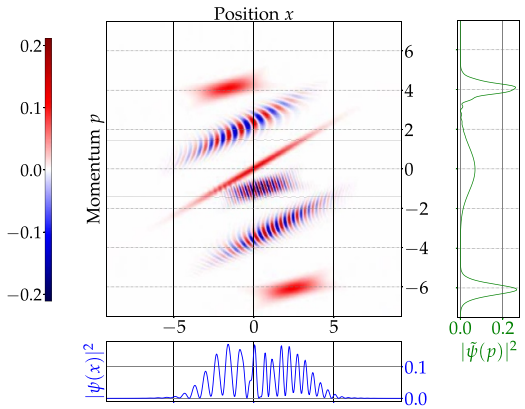

Figure 3. W's elementary phase space interference fringes [4, 7, 28] are roughly described by equation (3) but tend to be curved when created between two peaks of unequal shape (see fringes centered on $(-1,2)$ and $(2,-3)$) whereas peaks of equal shape create straight fringes (here at $(0,-1)$).

4.1. Interference between pairs of peaks

To theoretically underpin that the coherences between comb-state peaks gives rise to the observed formation of lines in phase space, we will now isolate the pertinent trigonometric terms that are responsible for the observed phenomena.

W for a 'Schródinger cat' state formed from two squeezed states $G(x,p) = \pi^{-1}\mathrm{e}^{-x^2/\xi^2-p^2\xi^2}$, with squeezing parameter ξ, according to equation (2), has the simple form

$$W(x,p) = \frac{G(x-\Delta x/2,p)+G(x+\Delta x/2,p)}{2} \tag{3a}$$

$$+\ G(x,p)\cos(p\Delta x)\,. \tag{3b}$$

This approximation for the description of a pair of peaks shows that they form an interference pattern (3*b*) of peak-width, halfway between peaks, with fringes whose spatial frequency ($k\sim p$) is proportional to the interpeak distance Δx, (see expression (3*b*) and appendix 'Wigner distribution fringes between two-peak combinations').

We emphasise that the interference pattern in phase space $\cos(p\Delta x)$ does not generally have such straight line behaviour, which requires equal shapes G of the constituent peaks. In general the associated interference fringes are curved, see figure 3.

To investigate the comb-state scenario we strip out the terms (3*a*) corresponding to the peaks themselves and only retain the terms (3*b*) describing phase space interference, compare figures 4(A) with (B).

We are left with the resulting simplified expression for a random comb-state's interference term

$$\mathcal{I} = \sum_{m=1}^{N-1}\sum_{n=m+1}^{N} \Lambda\left(x-\frac{X_m+X_n}{2}\right)\times\cos(p[X_m-X_n]-\phi_m+\phi_n)\,, \tag{4}$$

describing the effective overlap between peaks through Λ. The inter-peak distances, X_m-X_n, modulate the cosine-term in (4) analogously to expression (3*b*). Every peak at position X_m caries its own (constant) phase ϕ_m.

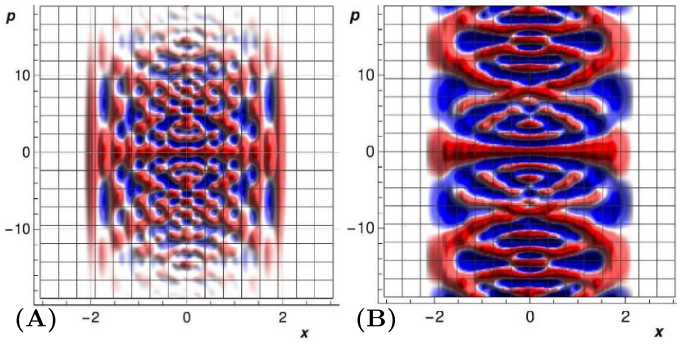

Figure 4. (A) W of comb-state versus (B) $\mathcal{I}$ of equation (4), with $\Lambda = 1$, with same locations and weights of peaks of comb-state as in figure 6(E). Both representations yield similar interference patterns: we conclude that coherences between peaks in comb-states are responsible for formation of lines.

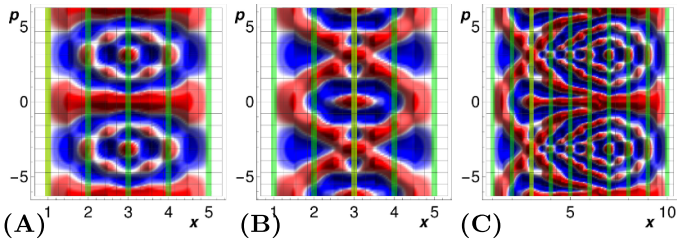

Figure 5. Plot of interference pattern $\mathcal{I}$ of equation (4) for equal equidistant peaks. The green strips indicate positions, X_m, of identical peaks. (A), all relative phases are zero: eye-patterns form. (B), phase of the central peak ($x = 3$) is shifted by π and (C) phase of the third peak, at position $x = 3$, is shifted by π: these randomising phase shifts lead to the formation of lines ((B)–(C)); also see appendix 'Eyes of varying orders'.

Numerically, whenever W (generated from peaks as in figures 6 and A.12) forms lines, then so does a plot of expression (4), figure 4 is a typical example.

Yet, we did not manage to extract an analytical expression that obviously displays the fact that formation of straight lines with positive values is encoded in (4), we therefore now discuss the emergence of straight lines due to random comb-states qualitatively instead.

4.2. Interference in combs of peaks

In figures 5(A) and 6(A) we observe that more symmetrical comb-states with fixed peak-to-peak distances and fixed constant phase across all peaks do not form straight lines in phase space, also see appendix 'Eyes of varying orders'.

When these comb-states are sufficiently randomized, however, they exhibit formation of straight lines in phase space, see figures 5(B), (C) and 6(D), (E). Additionally, we observe that imprinting completely random phases on each peak or shifting their individual momenta randomly (but moderately) or changing their relative weights randomly (but moderately) does not destroy the formation of straight lines in phase space (see appendices 'Randomized momenta: single eyes and triangle lines' and 'Randomized phases'): the formation of straight lines in phase space from randomized comb-states is a stable phenomenon.

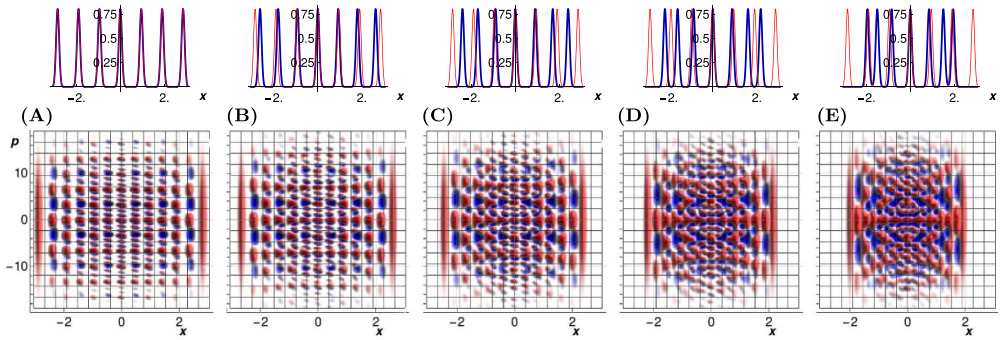

Figure 6. Randomized comb-state and associated Wigner distributions: $P(x)$ (top row) of a 7-peak state with constant peak-to-peak spacing (red curves) gets increasingly squashed towards the centre ((A)–(E)) reducing the peak-to-peak distances (blue curves). The resulting comb-states, randomized in interpeak distances, form Wigner distributions $W(x,p)$ that develop lines crisscrossing phase space (bottom row).

This stability can be understood from the functional form of the interference pattern $\mathcal{I}$. For example, shifts of a local phase ϕ_m entail a 'holistic effect' since several terms in equation (4) are affected in a synchronized fashion (see figure 5), thus interference patterns are modified smoothly rather than abruptly.

We find that for randomized comb-states the formation of lines in phase space is generic, see figure A.12, and that the formation of eye patterns occurs most clearly when locally concave comb-states form, see figure A.12(D), (E) and 8(B)–(D), and appendix 'Eyes of varying orders'.

4.3. Line formation in random potentials

Evolution in random potentials $V(x)$ is an obvious candidate for the synthesis of random comb-states. Here we create $V(x)$ from random Fourier series.

We commonly observe the formation of lines in phase space, see figure 7 (A) for a representative example.

Additionally, for a more symmetrical comb-state with a convex peak-weighting distribution, eyes form in phase space as well, see figure 7 (B).

5. Nonlinear systems

5.1. Line formation in free nonlinear systems

For the free ($V=0$) Schrödinger equation (1) of order three ($\epsilon=2$) with attractive nonlinearity, $\gamma>0$, it is known that initial states

$$\psi(x,0)=\frac{\mathrm{sech}(x)}{\sqrt{2}}\text{ with }\gamma=2N^2, N=1,2,3,\ldots \tag{5}$$

give rise to breather solutions with up to $N+1$ peaks and repetition period $T=\frac{\pi}{2}$ [29]. Their associated Wigner distributions W can display straight lines and ringed 'eye' shapes in phase space, see figure 8.

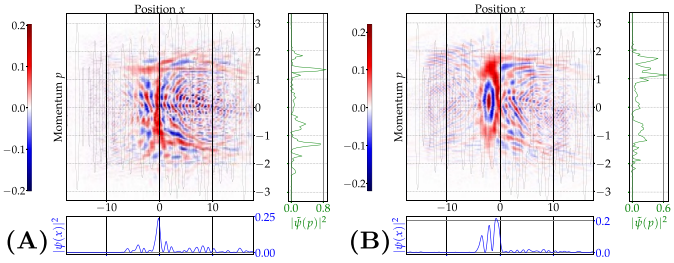

Figure 7. Random comb-states form in a random potential giving rise to lines across phase space and the formation of 'eye' patterns.

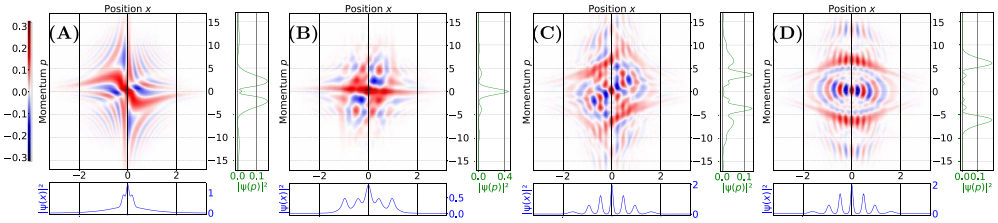

Figure 8. Wigner distributions evolved from initial sech-state (5) with $\gamma = 128$ ($N = 8$): (A) $t = 0.10$, (B) $t = 0.31$, (C) $t = 0.76$, and (D) $t = 0.79$. Note the formation of zero lines (white) in (A) and positive (red) straight lines throughout. In (B), (C) and (D) a regular array of peaks in the position distribution $P(x)$ which, in (C) and (D), coincides with a concave momentum distribution $\tilde{P}(p)$, giving rise to the formation of 'double-eye' patterns, compare figure A.12(E).

Straight lines also form for generic initial conditions which in the free case ($V = 0$) lead to evolution fulfilling the 'soliton resolution conjecture' [30]. The lines only form initially, while the radiative background and pre-solitonic peaks still overlap, see figure 9 for an example. This finding applies to wide classes of NLSEs as long as the interactions are attractive ($\gamma > 0$), see figure A.13.

In the case of repulsive interactions a confining potential is needed to trap the system state such that it self-interferes, forming comb-states with straight lines in phase space, see figure A.14.

5.2. *Line formation in trapped nonlinear systems*

Straight lines form repeatedly, we believe in perpetuity, when we confine the spread of the wave function by an external trapping potential since it traps the radiative background [30]. For an example see the bottom row of figure 10. Lines can form for nonlinear systems with different orders $\epsilon + 1$, see figure A.13.

We hope the reader finds our conjecture plausible that the formation of slightly randomized peaks is responsible for the formation of straight line patterns in phase space.

Whereas line formation is enhanced by the presence of attractive nonlinear interactions, figure 10, it can be present even for repulsive interactions ($\gamma < 0$) if a confining potential traps the state such that comb-states can form, see appendix 'Repulsive nlse'.

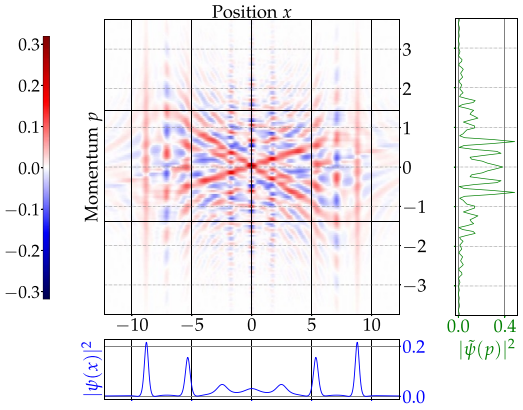

Figure 9. In a 'dam break scenario' comb-states form resulting in the formation of lines in phase space. Here, for a linear increase in nonlinearity ($\epsilon = 2$) such that $\gamma(t) = 150$ at $t = 5.75$, starting from $\gamma(t = 0) = 0$, and an initial 'straight-wall' state $\psi_0 = \exp[-32(x/5\pi)^{18}]/\sqrt{5\pi 2^{2/3}\Gamma(19/(18))}$.

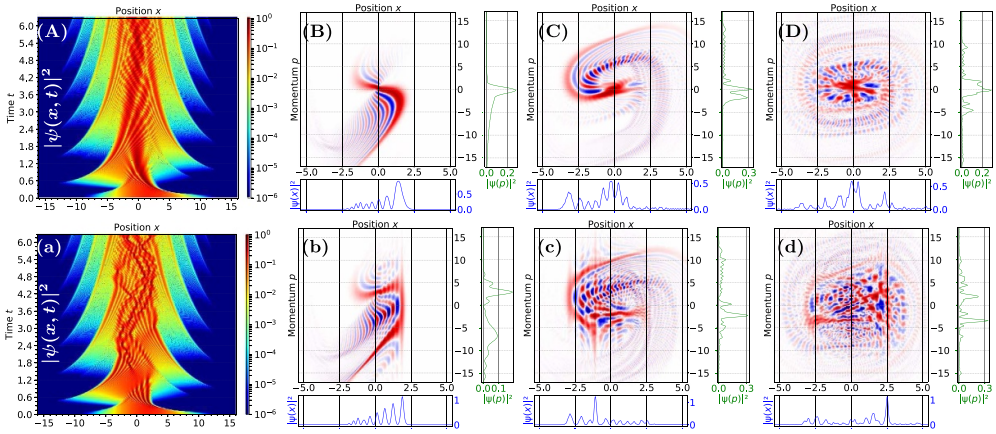

Figure 10. Enhanced line formation with attractive interaction: The initial state $\psi_0(x) = 0.43\exp[-(x-2)^2/19]$ evolves in the potential $V(x) = \frac{1}{10}x^4$ without, ($\gamma = 0$) top row ((A)–(D)), and in the presence of attractive interaction ($\gamma = 50$ and $\epsilon = 2$) bottom row ((a)–(d)). The spatial probability density $|\psi(x,t)|^2$, (A) and (a), shows dynamics dominated by oscillations due to the potential's confining forces. The associated Wigner distributions (using the same colouring as in figure 8), at times (B) and (b) $t = 0.55$, (C) and (c) $t = 1.76$, and (D) and (d) $t = 4.52$, prominently display straight lines crisscrossing phase space for the nonlinear case (b)–(d) whereas only weak lines form in the linear case, also see appendix 'Repulsive nlse'.

6. Conclusions

We have established that the states of many different types of quantum systems display formation of *positive* lines criss-crossing phase space; such lines cannot form in classical systems.

The formation of these lines is a robust phenomenon.

It will be interesting to see whether in higher-dimensional systems similar 'pencils' form in phase space.

The presence of attractive nonlinear interactions enhances the formation of lines criss-crossing phase space.

We moreover speculate that the formation of these lines might be able to illuminate the formation of rogue waves in nonlinear systems [13], using the phase space perspective.

Lines can also occur in linear or repulsive systems, if the state is confined by a trapping potential.

We expect that it should be possible to experimentally detect such lines through the detection of large peaks in measurements of suitably rotated quadratures and in quantum state reconstruction experiments [8, 9].

Data availability statement

The data that support the findings of this study are available upon reasonable request from the authors.

Acknowledgments

O S is extremely grateful to Denys Bondar for sharing his Python code on GitHub and his patient explanations on how to use it. He also appreciates the hospitality of the National Center for Theoretical Sciences during his stay in Hsinchu. This work is partially supported by the Ministry of Science and Technology of Taiwan (Nos. 108-2923-M-007-001-MY3 and 110-2123-M-007-002), Office of Naval Research Global, the International Technology Center Indo-Pacific (ITC IPAC) and Army Research Office, under Contract No. FA5209-21-P-0158, and the collaborative research program of the Institute for Cosmic Ray Research (ICRR) at the University of Tokyo.

Appendix. On the formation of lines in quantum phase space

Ole Steuernagel, Popo Yang and Ray-Kuang Lee

Wigner distribution fringes between two-peak combinations

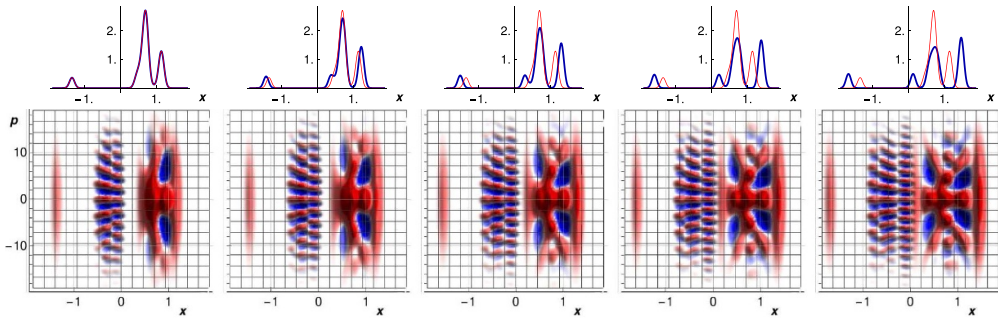

Figure A.11. Interference fringes in phase space for a two-peaked state form midway between wave function peaks and at a spatial frequency proportional to the interpeak distance, compare equation (3*b*). Here a distribution which is roughly concentrated in two spatial locations ($x<0$ versus $0<x$) (see $P(x)$ top row) displays simple interference in the region $-1<x<0$ [see $W(x,p)$ bottom row], which is graded (the spatial frequency increases from $x=-1$ to $x=0$) since $P(x)$ for positive values of x is spatially spread out. The phase space structure for the positive region, $x>0$, arises from the coherence of the three peaks located in that region. Therefore, the positive region by itself provides a simple and illustrative case for how lines crisscrossing phase space form.

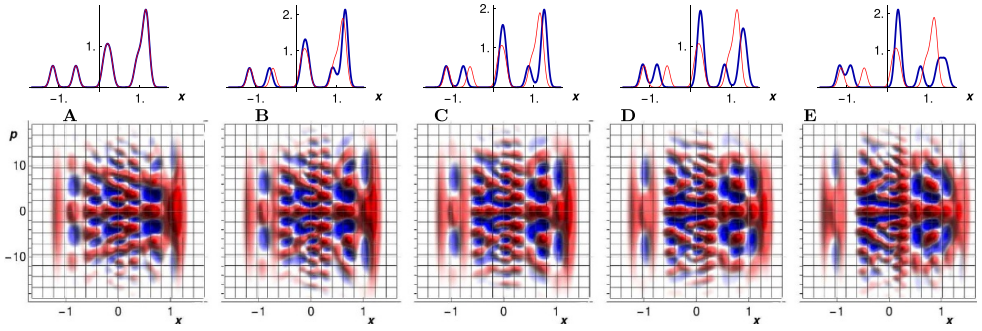

Figure A.12. Random 7-peak comb-states and associated Wigner distributions: $P(x)$ (top row) of states with 7 equally weighted peaks which are randomly distributed in position (and thus coalescing into 4 or 5 humps) are shown together with the associated Wigner distributions $W(x,p)$ (bottom row). $W(x,p)$ displays straight lines crisscrossing phase space. Panels (D) and (E) show a 'double-eye' pattern (bottom row) due to the concave arrangement of the weights of the last three (rightmost) humps (top row).

NLSEs of different orders

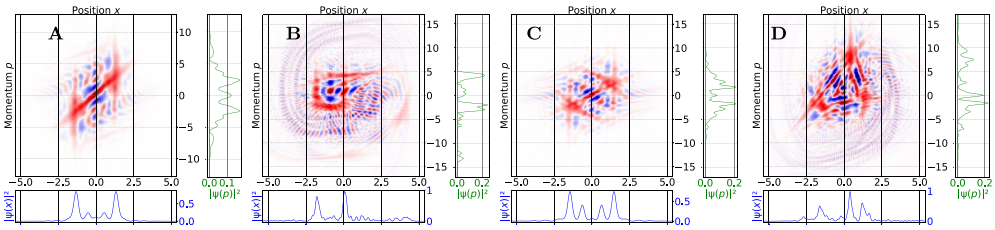

Figure A.13. Wigner distributions for NLSE systems (1) with varied order $\epsilon+1$, nonlinearity γ and potential V show formation of lines in phase space: from an initial squeezed state of the form $\psi_0(x) = 0.43\exp[-(x-x_0)^2/19]$, we show the time evolved state for A $\epsilon = 0.5, \gamma = 40, V = 0, x_0 = 0, t = 1.5$, B $\epsilon = 0.5, \gamma = 40, V = x^4/10, x_0 = 2, t = 2.7$, C $\epsilon = 1, \gamma = 40, V = 0, x_0 = 0, t = 1.38$, and D $\epsilon = 3, \gamma = 40, V = x^4/10, x_0 = 2, t = 2.0$.

Repulsive nlse

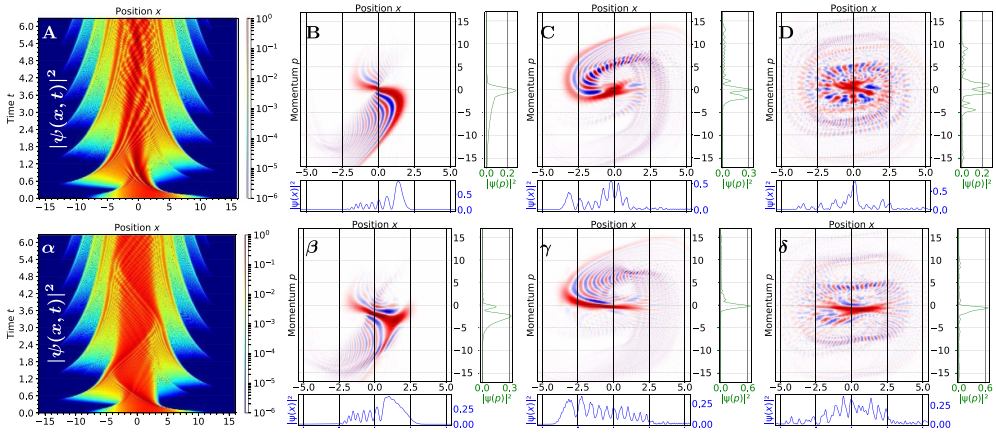

Figure A.14. Suppressed line formation in phase space for repulsive NLSE: top row: panels for linear Schrödinger equation, ($V(x) = \frac{1}{10}x^4$, $\psi_0(x) = 0.43\exp[-(x-2)^2/19]$, $\gamma = 0$), copied over from figure 10. Bottom row with same parameters except for repulsive interaction ($\gamma = -50$ and $\epsilon = 2$). Evolved Wigner distribution at various times: B and $\boldsymbol{\beta}$ at $t = 0.55$, C and $\boldsymbol{\gamma}$ at $t = 1.76$, and D and $\boldsymbol{\delta}$ at $t = 4.61$. Attractive NLSEs ($\gamma > 0$) tend to display enhanced line formation, repulsive NLSEs ($\gamma < 0$) tend to display suppressed line formation.

Eyes of varying orders

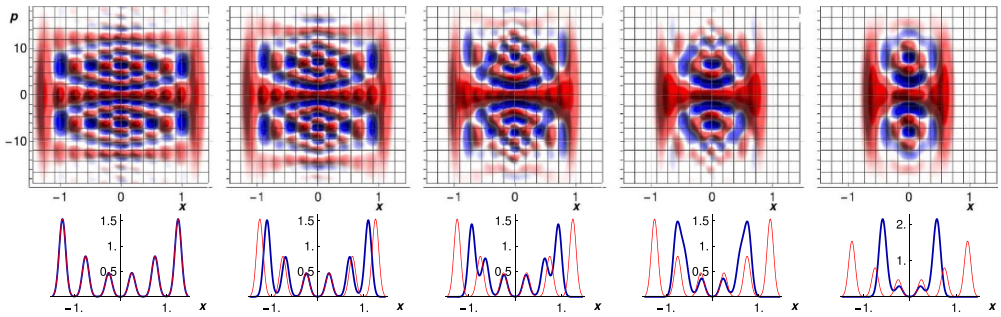

Figure A.15. 'Double eye' pattern in phase space: comb-states with a concave arrangement of an even number of peaks (see $P(x)$ in bottom row) yield a characteristic double eye interference pattern (with a negative (blue) centre) with varying order of the number of concentric rings within each eye (see $W(x,p)$ in top row). Inter-peak phase differences are zero whereas distances are not constant.

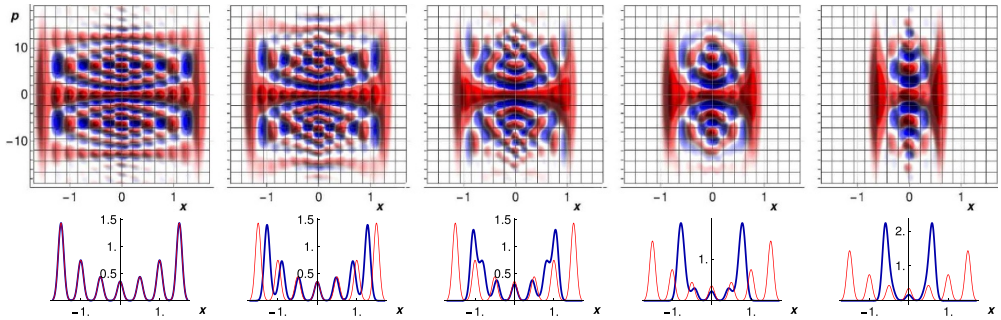

Figure A.16. 'Double eye' pattern in phase space: similar to figure A.15, but for an odd number of peaks, yielding positive (red) centres in $W(x,p)$. Inter-peak phase differences are zero whereas distances are not constant.

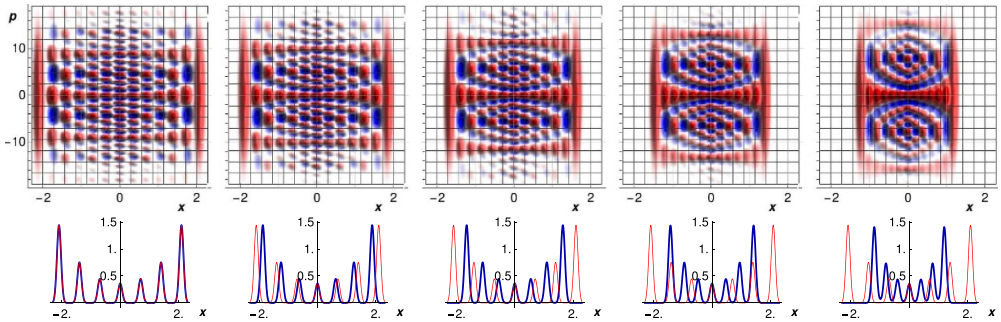

Figure A.17. 'Eye' pattern in phase space: similar to figure A.16, but for peaks which are equidistant to each other.

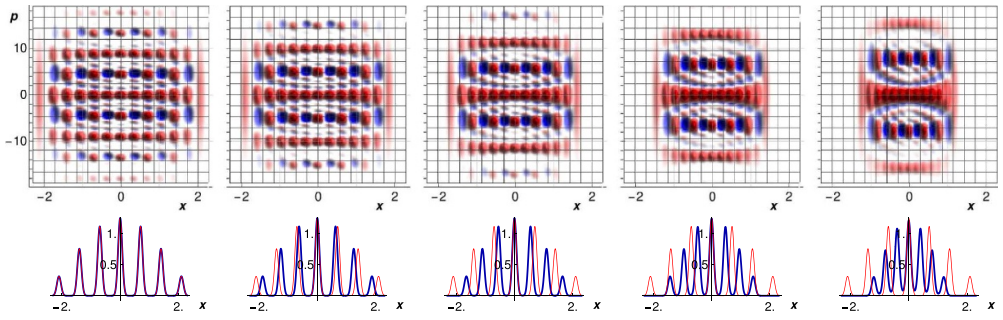

Figure A.18. 'Eye' pattern in phase space: similar to figure A.17, but for peaks with a convex weighting distribution. In this convex case the formation of eye patterns is less 'clean' than in the concave case of e.g. figure A.17.

Randomized momenta: single eyes and triangle lines

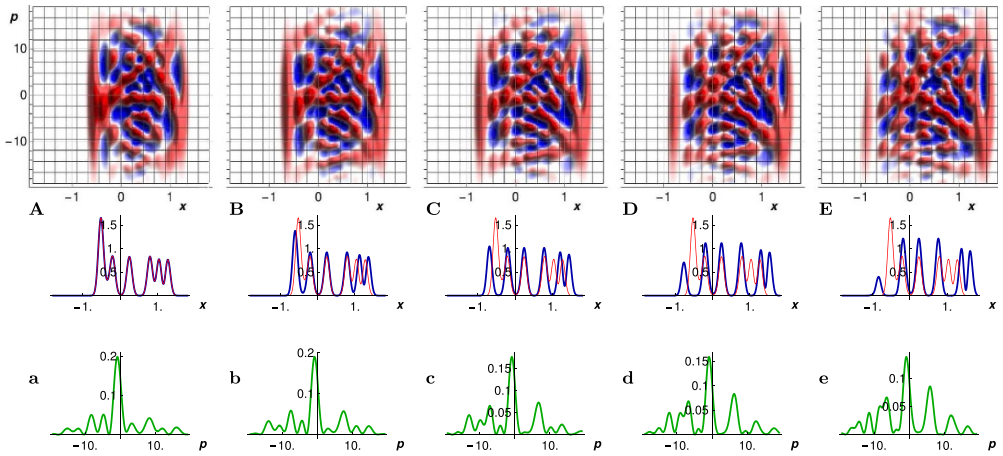

Figure A.19. 'Single eye' pattern in phase space: here, comb-states for which not only the peak positions (see $P(x)$ in (A)–(E)) but also the mean momenta of the peaks are randomized (see $\tilde{P}(p)$ in a–e is not an even function). This demonstrates that also single eye patterns can form (see $W(x,p)$ in (A) and (B)). Triangle line arrangements, e.g. in panel (E), resemble those in figure 10(d) and figure A.13(D).

Randomized phases

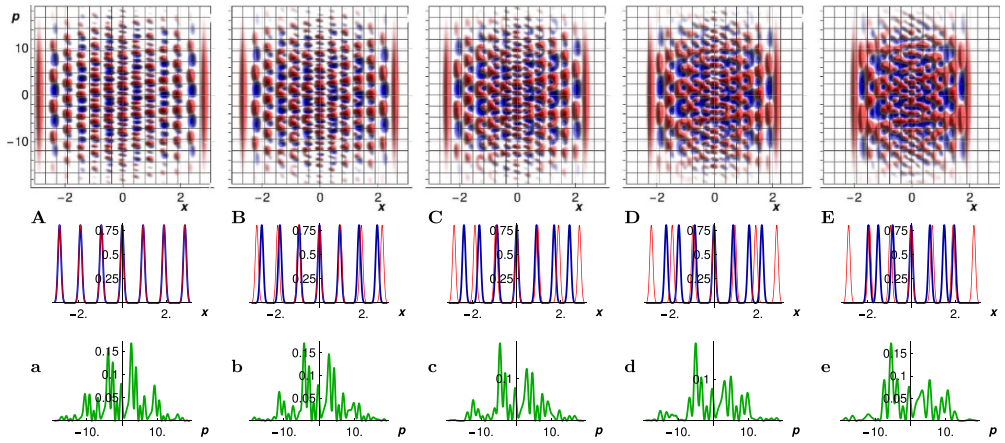

Figure A.20. Comb-states with randomized phases form lines in phase space: $P(x)$ in (A)–(E) has the same shape as in figure 6 but since every peak carries a completely random phase the momentum distributions $\tilde{P}(p)$ in (a)–(e) are not even functions any more, yet, $W(x,p)$ forms lines in phase space.

ORCID iDs

Ole Steuernagel https://orcid.org/0000-0001-6089-7022
Ray-Kuang Lee https://orcid.org/0000-0002-7171-7274

References

[1] Korsch H J and Berry M V 1981 Evolution of Wigner's phase-space density under a nonintegrable quantum map *Phys. D Nonl. Phen.* **3** 627–36
[2] Dragoman D and Dragoman M 1997 Phase space characterization of solitons with the Wigner transform *Opt. Commun.* **137** 437–44
[3] Torres-Vega G, Møller K B and Zuñiga-Segundo A 1998 Role that separatrices and stochastic webs play in quantum dynamics *Phys. Rev.* A **57** 771
[4] Zurek W H 2001 Sub-Planck structure in phase space and its relevance for quantum decoherence *Nature* **412** 712–17
[5] Gao H, Tian L and Barbastathis G 2014 Hamiltonian and phase-space representation of spatial solitons *Opt. Commun.* **318** 199–204
[6] Martins A X, Paiva R A S, Petronilo G, Luz R R, Amorim R G G, Ulhoa S C and Filho T M R 2020 Analytical solution for the Gross–Pitaevskii equation in phase space and Wigner function *Adv. High Energy Phys.* **2020** 1–6
[7] Wigner E 1932 On the quantum correction for thermodynamic equilibrium *Phys. Rev.* **40** 749–59
[8] Hofheinz M *et al* 2009 Synthesizing arbitrary quantum states in a superconducting resonator *Nature* **459** 546–9
[9] Kurtsiefer C, Pfau T and Mlynek J 1997 Measurement of the Wigner function of an ensemble of helium atoms *Nature* **386** 150–3
[10] We use a unit-free description, setting $\hbar = 1$ and particle mass $M = 1$. For details see, e.g. [17]. Equation (1) is norm conserving [30]

[11] Zabusky N J and Kruskal M D 1965 Interaction of "solitons" in a collisionless plasma and the recurrence of initial states *Phys. Rev. Lett.* **15** 240
[12] Kivshar Y S and Agrawal G P 2003 *Optical Solitons: From Fibers to Photonic Crystals* (New York: Academic)
[13] Soto-Crespo J M, Devine N and Akhmediev N 2016 Integrable turbulence and rogue waves: breathers or solitons? *Phys. Rev. Lett.* **116** 103901
[14] Marcucci G, Pierangeli D, Agranat A J, Lee R-K, DelRe E and Conti C 2019 Topological control of extreme waves *Nat. Commun.* **10** 1–8
[15] The associated energy expression is [30]

$$\mathcal{H} = \int \mathrm{d}x \left[\frac{1}{2} \left| \frac{\partial \psi}{\partial x} \right|^2 + V|\psi^2| - \frac{2\gamma}{\epsilon+2} |\psi(x,t)|^{\epsilon+2} \right], \tag{6}$$

our description is unit-free
[16] We investigate NLSEs with ϵ varying from 0.5 to 3.5, for $\epsilon = 2$ this is the time-dependent Gross–Pitaevskii equation, for large nonlinearities blowup instabilities can occur [30] (arXiv:2010.07654)
[17] Oliva M and Steuernagel O 2019 Dynamic shear suppression in quantum phase space *Phys. Rev. Lett.* **122** 020401
[18] Oliva M, Kakofengitis D and Steuernagel O 2017 Anharmonic quantum mechanical systems do not feature phase space trajectories *Physica* A **502** 201–10
[19] Steuernagel O 2014 Equivalence between free quantum particles and those in harmonic potentials and its application to instantaneous changes *Eur. Phys. J. Plus* **129** 114
[20] Averbukh I S and Perelman N F 1989 Fractional revivals: universality in the long-term evolution of quantum wave packets beyond the correspondence principle dynamics *Phys. Lett.* A **139** 449–53
[21] Robinett R W 2004 Quantum wave packet revivals *Phys. Rep.* **392** 1–119
[22] Infeld E 1981 Quantitive theory of the Fermi–Pasta–Ulam recurrence in the nonlinear Schrödinger equation *Phys. Rev. Lett.* **47** 717
[23] Trillo S and Wabnitz S 1991 Dynamics of the nonlinear modulational instability in optical fibers *Opt. Lett.* **16** 986–8
[24] Hillery M, O'Connell R F, Scully M O and Wigner E P 1984 Distribution functions in physics: fundamentals *Phys. Rep.* **106** 121–67
[25] We use a unit-free description, setting $\hbar = 1$ and particle mass $M = 1$. For details see, e.g. [17]
[26] Zachos C K, Fairlie D B and Curtright T L 2005 *Quantum Mechanics in Phase Space* (Singapore: World Scientific)
[27] Oliva M and Steuernagel O 2019 Quantum Kerr oscillators' evolution in phase space: Wigner current, symmetries, shear suppression and special states *Phys. Rev.* A **99** 032104
[28] Schleich W P 2001 *Quantum Optics in Phase Space* (Berlin: Wiley-VCH)
[29] Schrader D 1995 Explicit calculation of N-soliton solutions of the nonlinear Schroedinger equation *IEEE J. Quant. Electr.* **31** 2221–5
[30] Tao T 2009 Why are solitons stable? *Bull. Am. Math. Soc.* **46** 1–33